

Both Functional LT β Receptor and TNF Receptor 2 Are Required for the Development of Experimental Cerebral Malaria

Dieudonné Togbe^{1,9}, Paulo Loureiro de Sousa^{2,9}, Mathilde Fauconnier¹, Victorine Boissay¹, Lizette Fick³, Stefanie Scheu⁴, Klaus Pfeffer⁴, Robert Menard⁵, Georges E. Grau⁶, Bich-Thuy Doan², Jean Claude Beloeil², Laurent Renia^{6,8}, Anna M. Hansen⁶, Helen J. Ball⁶, Nicholas H. Hunt⁶, Bernhard Ryffel^{1*}, Valerie F. J. Quesniaux^{1*}

1 University of Orléans and CNRS, Molecular Immunology and Embryology UMR6218, Orleans, France, **2** CNRS CBM (Centre de Biophysique Moléculaire), Orleans, France, **3** Institute of Infectious Disease and Molecular Medicine, Cape Town, South Africa, **4** University of Duesseldorf, Duesseldorf, Germany, **5** Pasteur Institute Paris, Paris, France, **6** The University of Sydney, Department of Pathology, Camperdown, Australia, **7** Institut Cochin, Université Paris Descartes, CNRS (UMR 8104), Paris, France, **8** Inserm, U567, Paris, France

Abstract

Background: TNF-related lymphotoxin α (LT α) is essential for the development of *Plasmodium berghei* ANKA (PbA)-induced experimental cerebral malaria (ECM). The pathway involved has been attributed to TNFR2. Here we show a second arm of LT α -signaling essential for ECM development through LT β -R, receptor of LT α 1 β 2 heterotrimer.

Methodology/Principal Findings: LT β R deficient mice did not develop the neurological signs seen in PbA induced ECM but died at three weeks with high parasitaemia and severe anemia like LT α β deficient mice. Resistance of LT α β or LT β R deficient mice correlated with unaltered cerebral microcirculation and absence of ischemia, as documented by magnetic resonance imaging and angiography, associated with lack of microvascular obstruction, while wild-type mice developed distinct microvascular pathology. Recruitment and activation of perforin⁺ CD8⁺ T cells, and their ICAM-1 expression were clearly attenuated in the brain of resistant mice. An essential contribution of LIGHT, another LT β R ligand, could be excluded, as LIGHT deficient mice rapidly succumbed to ECM.

Conclusions/Significance: LT β R expressed on radioresistant resident stromal, probably endothelial cells, rather than hematopoietic cells, are essential for the development of ECM, as assessed by hematopoietic reconstitution experiment. Therefore, the data suggest that both functional LT β R and TNFR2 signaling are required and non-redundant for the development of microvascular pathology resulting in fatal ECM.

Citation: Togbe D, Loureiro de Sousa P, Fauconnier M, Boissay V, Fick L, et al. (2008) Both Functional LT β Receptor and TNF Receptor 2 Are Required for the Development of Experimental Cerebral Malaria. PLoS ONE 3(7): e2608. doi:10.1371/journal.pone.0002608

Editor: Denise L. Doolan, Queensland Institute of Medical Research, Australia

Received: March 28, 2008; **Accepted:** June 4, 2008; **Published:** July 9, 2008

Copyright: © 2008 Togbe et al. This is an open-access article distributed under the terms of the Creative Commons Attribution License, which permits unrestricted use, distribution, and reproduction in any medium, provided the original author and source are credited.

Funding: Work supported by CNRS, the interdisciplinary program MIE from the French Research Minister, and European FP6 MPCM project.

Competing Interests: The authors have declared that no competing interests exist.

* E-mail: bryffel@cns-orleans.fr (BR); quesniaux@cns-orleans.fr (VFJQ)

These authors contributed equally to this work.

Introduction

Cerebral malaria is a frequent cause of death in children and young adults infected with *Plasmodium falciparum* [1], which is characterized by the sequestration of parasitized erythrocytes in cerebral blood vessels [2,3]. TNF has been originally implicated in pathogenesis of the neurological complication [4]. In patients with cerebral malaria disease severity has been correlated with TNF serum levels [5–7]. In experimental murine malaria the administration of TNF neutralizing antibodies prevented experimental cerebral malaria (ECM) [8]. Mice with a combined inactivation of TNF and LT α were to be resistant to ECM development [9]. Recent data suggest that LT α rather than TNF is responsible for the development of microvascular damage resulting in the neurological malaria complication [10].

Lymphotoxin alpha is a member of TNF superfamily and the closest TNF relative. It exists as a soluble homotrimer (LT α 3) or forms membrane-bound heterotrimers with the membrane associated lymphotoxin beta (LT β) [11,12]. Both homotrimeric TNF and LT α 3 interact with two receptors, TNFR1 (CD120 α) and TNFR2 (CD120 β), whereas membrane bound LT α β heterotrimers function through the engagement of LT β R [13,14]. LT β R binds not only LT α β heterotrimers but also LIGHT homotrimers, another TNF family member. Both LIGHT and LT α 3 bind herpes virus entry mediator (HVEM), a fourth member of TNFR superfamily. The role of soluble LT α 3, of LT α β and LIGHT in pathogenesis is not fully understood.

Mice with complete inactivation of TNF or TNFR1 gene are unable to mount a protective response against various pathogens [15], but develop ECM, while TNFR2 deficient mice are resistant to

ECM development [16]. In order to assess the role of membrane $LT\alpha\beta$ heterotrimer signaling we studied ECM development in $LT\beta R$ deficient mice [17] and further extended the investigation to LIGHT, using LIGHT gene deficient mice [18].

Here we report that absence of $LT\beta R$ prevented ECM development. Magnetic resonance imaging (MRI) and angiography (MRA) were used to verify the lack of ischemia and microvascular pathology in these mice. Therefore, the data suggest that both functional $LT\beta R$ and TNFR2 axis are required for the development of microvascular pathology resulting in fatal ECM. The disruption of either axis prevents cerebral microvascular disease.

Results

Disruption of $LT\beta R$ signaling protects from fatal ECM development

$LT\alpha$ and TNFR2 signaling have been shown to be critical for *Plasmodium berghei* ANKA (PbA) induced ECM, as mice deficient for either $LT\alpha$ or TNFR2 are resistant to cerebral malaria, while TNFR1 is dispensable [10,16]. Since $LT\alpha$ exists either as soluble homotrimer or heterotrimer in association with membrane bound $LT\beta$, we asked whether signaling of membrane $LT\alpha\beta$ through $LT\beta R$ may be involved in ECM development.

We show here that $LT\beta R$ deficient mice did not develop ECM and survived more than 20 days, while C57BL/6J wild type mice developed typical neurological signs of CM, including postural disorders, ataxia, impaired reflexes and loss of grip strength, progressive paralysis and coma, and succumbed within a week after infection with 5–10% of parasitized erythrocytes (Figure 1A). In order to compare directly the requirement for different members of the TNF family, mice deficient for TNF, $LT\alpha$, $LT\beta$, LIGHT, TNFR1 or TNFR2 were infected with blood stage PbA. $LT\alpha$ and TNFR2 deficient mice resisted to ECM development (Figure 1B, C), with no neurological signs up to day 22–25, at which time they succumbed of high parasitaemia and anemia (Figure 1D,E and data not shown), consistent with published data [16]. In contrast, mice deficient for TNF, LIGHT or TNFR1 developed neurological signs and succumbed to ECM within 7–10 days (Figure 1B, C). $LT\beta$ deficient mice were more susceptible than $LT\alpha$ deficient mice, although they did not show neurological signs in the first week of infection, and developed slightly higher parasitemia and anemia than wild-type mice (Figure 1D, E). Therefore, our data demonstrate that $LT\beta R$ signaling is necessary for ECM development.

Absence of ECM signs in $LT\beta R$ deficient mice correlates with MRI and MRA based morphological analysis

Magnetic resonance imaging (MRI) is a non-invasive tool to investigate neurological disease processes in humans. In the murine experimental cerebral malaria model using MRI allow a semi-quantitative analysis of brain swelling, microvascular pathology due to obstruction of small vessels with parasitized erythrocytes and leukocytes endothelial damage, edema and focal ischemia [10,16,19]. Mice deficient for $LT\beta R$, $LT\alpha\beta$ -deficient mice used as ECM resistant controls, and wild-type C57BL/6 or TNF-deficient mice used as ECM sensitive controls, were examined by MRI at day 7, when wild-type mice are dying with acute ECM, while $LT\beta R$ and $LT\alpha\beta$ -deficient mice were all alive without neurological signs.

Typical MRI and MRA images of uninfected and infected mice are shown in Figure 2A and 2B, respectively. While wild-type C57BL/6 and TNF-deficient mice presented signs of ischemic brain damage and vascular blood flow perturbations upon blood stage PbA infection, $LT\alpha\beta$ and $LT\beta R$ deficient mice displayed a normal MRI. Overall, mice deficient for $LT\alpha\beta$ ($n = 6$) or $LT\beta R$

($n = 7$) showed unaltered MRI and MRA signals. By contrast, wild-type mice showed altered MRI, observable as a bilateral hyperintense signal at the corpus callosum and external capsule (Figure 2A), and a remarkable vascular blood flow perturbations was detected in wild-type mice (Figure 2B). In addition, brain swelling was observed in infected wild-type C57BL/6 mice during acute cerebral malaria. TNF deficient mice showed an intermediate phenotype with an altered MRI and MRA perturbation in infected mice analyzed. Non-infected wild-type or gene deficient mice presented normal MRI and MRA phenotype (Figure 2A, B). MRA 3D reconstructions available in supplementary data show the clear difference in brain blood flow between non infected wild-type mice (Video S1_B6_NI), 7 day PbA infected wild-type (Video S2_B6_PbA) and TNF-deficient mice (Video S3_TNF ko_PbA) on the one hand, and mice deficient for $LT\beta R$ (Video S4_LT $\alpha\beta$ ko_PbA) or $LT\alpha\beta$ (Video S5_LT βR ko_PbA), on the other hand.

Therefore, $LT\alpha\beta$ - $LT\beta R$ signaling is necessary to develop ischemic brain damage and vascular blood flow perturbations.

$LT\beta R$ deficient mice do not develop microvascular lesions

In order to validate functionally the data obtained by MRI, we investigated microvascular lesions in the brain. Microvessel obstruction and disruption, which leads to increased protein extravasation from the capillary bed, was quantified by Evans blue leakage into the tissue. PbA infected wild-type or TNF deficient mice showed a strong vascular leak of Evans blue, while mice deficient for $LT\alpha\beta$ or $LT\beta R$ had no discoloration of the brain parenchyma (Figure 3A), with limited Evans blue vascular leak (Figure 3B), suggestive of an intact blood-brain barrier.

Microscopically, the vascular leak is due to microvascular lesions in the brain with perivascular hemorrhage and intravascular accumulation of mononuclear cells and infected erythrocytes (Figure 3C), which was completely absent in $LT\alpha\beta$ and $LT\beta R$ deficient mice. The severity of microvascular obstruction and local hemorrhage in the brain were assessed semi-quantitatively, and clearly demonstrate significant differences. The information obtained by MRI was compared to that derived from the microscopic examination of the brain. There was a good agreement of the predicted brain pathology by MRI and microscopic investigation.

Since microvascular disease occurring in PbA infected mice presenting with CM is not limited to the brain, we also investigated the pulmonary microvascular beds. While the lungs of wild-type and TNF-deficient mice displayed congested septal capillaries, hemorrhages and interstitial edema, $LT\alpha\beta$ or $LT\beta R$ deficient mice had no evidence of microvascular pathology, with less erythrocytes in the alveoli (Figure 3E, G). However, wild-type, TNF, $LT\alpha\beta$ and $LT\beta R$ deficient mice had comparable thickening of alveolar septae (Figure 3F).

Therefore, the data suggest that disruption of $LT\alpha\beta$ – $LT\beta R$ signaling prevents microvascular pathology induced by PbA blood stage infection.

Reduced sequestration of effector T lymphocytes in the brain of PbA infected $LT\beta R$ deficient mice

Trafficking and recruitment of effector T lymphocytes into the brain are clearly necessary for the development of the pathology associated with ECM [20,21]. We next characterized brain-sequestered leukocytes, in wild-type and TNF deficient mice with severe neurological symptoms after PbA infection and in $LT\beta R$ or $LT\beta$ deficient mice at the same day after infection. Similar numbers of $CD4^+$ T cells were recovered from uninfected and infected wild-type mice, as well as from PbA infected TNF or $LT\beta$ deficient mice (Figure 4A, E). Interestingly, the strong increase in brain $CD8^+$ T cells seen in wild type or TNF deficient mice that

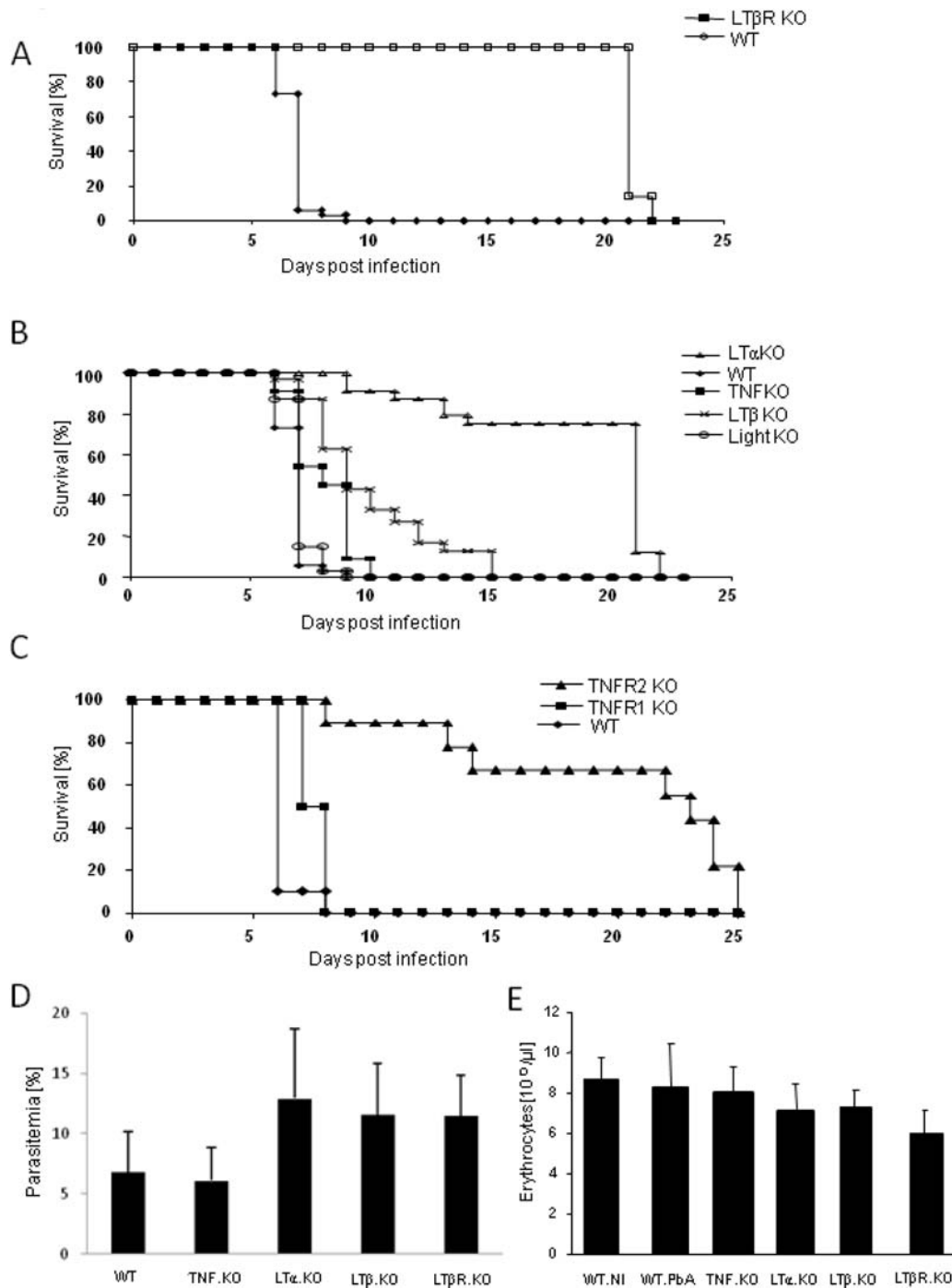


Figure 1. LTβR deficient mice do not develop PbA induced ECM. C57BL/6 (WT) and mice deficient for LTβR (A), LTα, LTβ, LIGHT or TNF (B), TNFR1 or TNFR2 (C) were infected with 10⁶ *P. berghei* ANKA parasitized red blood cells and their survival monitored daily. At day 7, parasitemia (D) was significantly increased in LTα, LTβ and LTβR-deficient mice ($p < 0.01$) and red blood cell counts (E) were significantly reduced in LTβR-deficient mice ($p < 0.0001$) and less so in LTα or LTβ deficient mice ($p < 0.01$). Results are from $n = 14-33$ mice per genotype pooled from five independent experiments. Logrank test analysis of the Kaplan-Meier curves indicated p values < 0.0001 for each genotype compared to WT, with the exception of LIGHT-deficient mice which was non significant (0.3) and TNF-deficient mice (< 0.05). doi:10.1371/journal.pone.0002608.g001

develop cerebral malaria was essentially absent in PbA-infected LTβR or LTβ deficient mice (Figure 4A, F). We then analysed the functional state and cytotoxic potential of brain-sequestered CD8⁺ T cells from PbA-infected mice (Figure 4B, G). Most brain CD8⁺ T cells expressed perforin in PbA-infected wild-type or TNF deficient mice, but ECM resistant LTβR deficient mice sequestered far less

perforin⁺ CD8 T lymphocytes (Figure 4B, G). Moreover, we show that LTβR or LTβ deficient mice have lower numbers of ICAM/CD54⁺ and CD69⁺ CD8 T cells than wild type or TNF deficient mice upon PbA infection (Figure 4C, D, H, I). LTβ deficient mice were only partially protected and succumbed to lethal ECM a few days later than the wild-type mice.

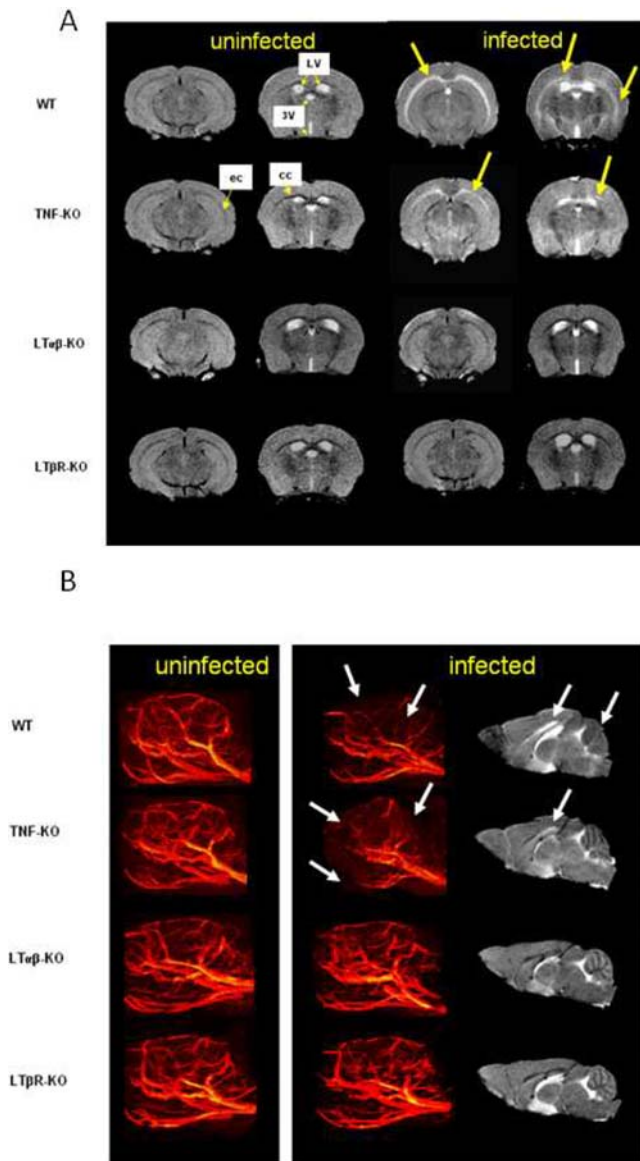


Figure 2. MRI analysis of Pba induced morphological changes.
A. MRI of uninfected and infected mice, 7 days post infection with 10^6 *P. berghei ANKA* parasitized red blood cells: Distinct anomalies are visible in C57BL/6 (WT) and TNF mice, namely edema formation, apparent as a bilateral hyperintense signal as indicated by arrows in the right 2 sets of photographs at the corpus callosum (c.c.) and external capsule (e.c.), while $LT\alpha\beta$ and $LT\beta R$ deficient mice do not show these alterations. LV and 3V indicate the lateral and third ventricles, respectively. Images correspond to the stereotaxic position Bregma -2.92 and -0.58 mm.
B. Magnetic Resonance Angiography: when compared to uninfected mice (left panel) vascular blood flow perturbations (shown by arrows) are evident in WT and TNF-KO mice, 7 days post infection with 10^6 *P. berghei ANKA* parasitized red blood cells, while $LT\alpha\beta$ and $LT\beta R$ deficient mice seem unaffected (middle panel). Sagittal MR images obtained from the same infected mice (right panel) indicate the main MRI alterations: oedema formation and cerebellar damage (shown by arrows). Brain swelling has been observed only in C57BL/6 and TNF-KO mice. MRA 3D reconstructions are shown in supplementary data.
 doi:10.1371/journal.pone.0002608.g002

In conclusion, these data suggest a pathogenic role of activated effector $CD8^+$ T lymphocytes recruited in brain of wild-type and TNF deficient mice developing ECM, whereas the ECM resistance in $LT\beta R$ deficient mice is associated with strongly reduced sequestration of $CD8^+$ T lymphocytes.

Parasitaemia is $LT\alpha\beta$ - $LT\beta R$ signaling independent

We then asked whether parasitaemia and anemia are influenced in the absence of $LT\beta R$ signaling. Parasitaemia was analyzed by flow cytometry using GFP transfected parasites [22]. Parasitaemia is usually low (less than 10%) at the time of ECM onset. Absence of $LT\beta R$ had no effect on parasitaemia as compared to wild-type mice at day 7 (Figure 5A). However, mice deficient for either $LT\alpha$ or $LT\beta R$ developed extremely high parasitaemia of about 70% by day 20 (Figure 5B), consistent with published data in $LT\alpha$ deficient mice [10].

The hematological investigations at 7 days after infection revealed distinct reductions of platelet counts in C57BL/6 mice as compared to non-infected mice (Figure 5C), as reported [23], and we show a similar thrombocytopenia in the ECM resistant $LT\beta R$ deficient mice (Figure 5D). The latter finding suggests that thrombocytopenia in $LT\beta R$ deficient mice is not an indicator of platelet sequestration in microvessels in this model.

The total white blood cell counts decreased after 7 days of Pba infection in wild type mice, and this was largely attributed to a decrease in lymphocytes (Figure 5E), while monocyte and neutrophil counts were essentially unaffected (data not shown). $LT\beta R$ deficient mice also experienced a marked decrease in lymphocyte counts (Figure 5F).

Finally, no significant anemia developed in wild-type mice 7 days post-infection, the erythrocyte count was still in the normal range (Figure 5G) as well as the hematocrit (Figure 5I) and hemoglobin concentrations (data not shown). Erythrocyte counts and hematocrit were slightly decreased on day 7 in $LT\beta R$ deficient mice (Figure 5H, J). The ECM resistant, $LT\beta R$ deficient mice further developed dramatic anemia (Figure 5H), similar to $LT\alpha$ deficient mice ($1.34 \pm 0.30 \times 10^6$ RBC/ μ L), and probably succumb of general hypoxia after 3 weeks.

In conclusion, the resistance to ECM development of $LT\alpha$ and $LT\beta R$ deficient mice was not attributable to decreased parasitaemia or thrombocytopenia, and the ECM resistant mice developed very high parasitaemia and died of severe anemia within 3 weeks.

Absence of $LT\beta R$ expression on stromal cells determines resistance to ECM

To assess the cellular source of $LT\beta R$ that mediates resistance toward ECM development, we generated bone marrow chimeric mice. Wild-type C57BL/6 and $LT\beta R$ deficient mice were lethally irradiated and engrafted with bone marrow from either C57BL/6 mice or $LT\beta R$ deficient mice [24,25]. After infection with 10^6 *P. berghei ANKA* parasitized erythrocytes, wild-type mice reconstituted with $LT\beta R$ deficient bone marrow died as rapidly as wild-type mice reconstituted with wild-type bone marrow (Figure 6A). In contrast, $LT\beta R$ deficient mice reconstituted with wild-type bone marrow displayed protection to ECM comparable to $LT\beta R$ deficient mice reconstituted with $LT\beta R$ deficient bone marrow, and further developed severe fatal anaemia, but no cerebral syndrome. Erythrocyte counts and hematocrit were already decreased on day 7 in $LT\beta R$ deficient mice reconstituted with either $LT\beta R$ deficient or wild-type bone marrow (Figure 6B,C), similar to non-reconstituted $LT\beta R$ deficient mice (Figure 5H, J). Platelet and lymphocyte count decrease seen 7 days after infection were largely dependent on the recipient mice (Figure 6D, E), and were similar to non-reconstituted mice (Figure 5C–F). Since the resistance of $LT\beta R$ deficient mice to ECM development was not corrected by wild-type bone marrow reconstitution, the data suggest that $LT\beta R$ expression on radioresistant, stromal probably endothelial cells determines the sensitivity to ECM and bone marrow cells from $LT\beta R$ can not transfer ECM resistance to sensitive wild-type mice.

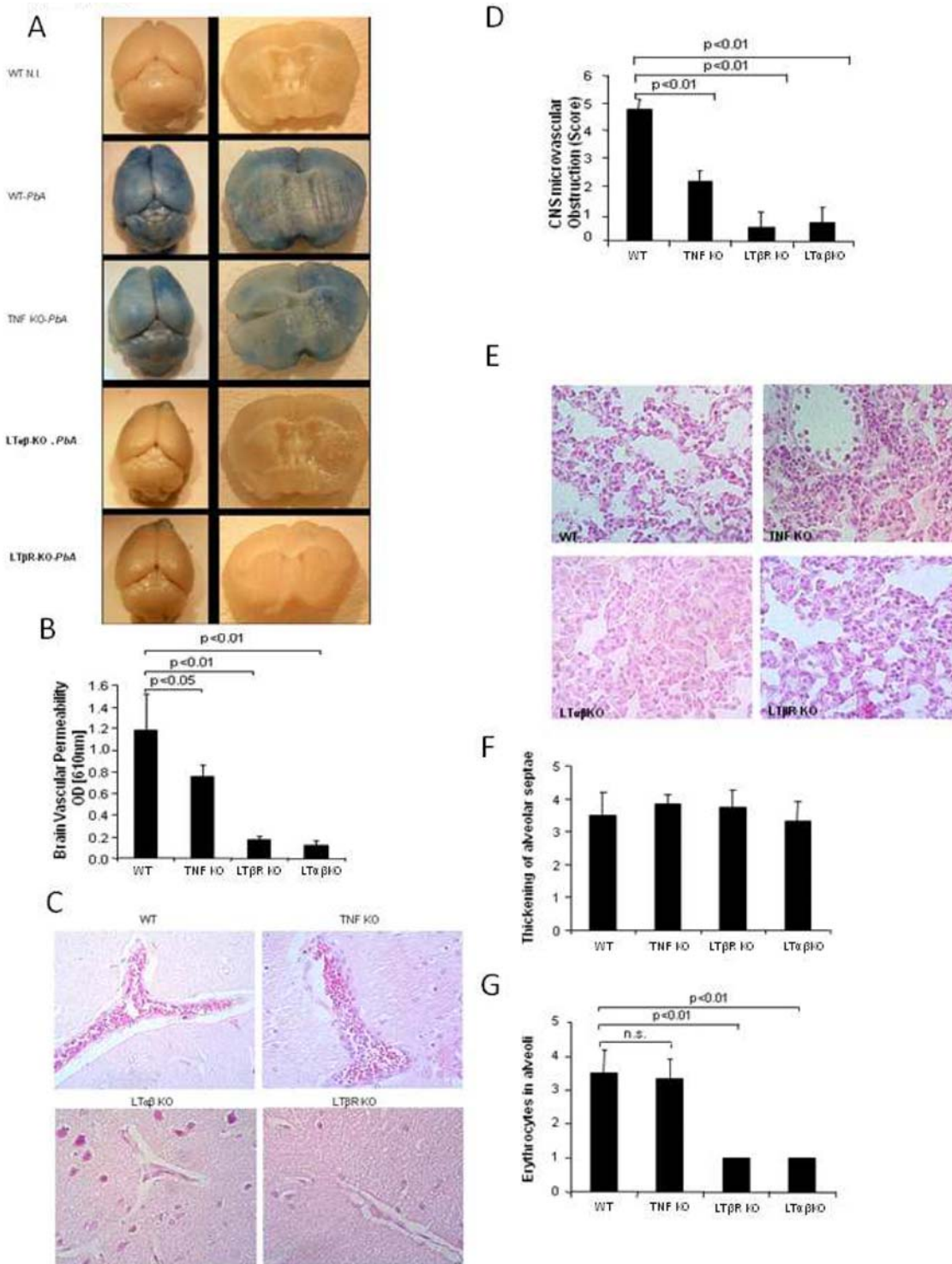


Figure 3. LTβR deficient do not develop ECM-associated brain vascular leakage. Vascular leak as assessed by the blue discoloration of the brain of wild-type control C57BL/6 (WT), TNF, LTα or LTβR deficient mice injected intravenously with 1% Evans blue on day 7 with severe ECM (A). Mice were infected with 10⁶ *P. berghei* ANKA parasitized red blood cells as in Fig. 1. Quantitative assessment of brain capillary permeability using Evans blue extravasation in formamide was measured by Absorbance at 610 nm in brain extract (B). Microvascular damage with mononuclear cell adhesion and perivascular hemorrhage in the brain of WT and TNF deficient mice, but not LTα, nor LTβR deficient, micrograph 400×, H&E stained brain sections (C). Semi-quantitative score of brain infiltration and hemorrhages (D). Microvascular damage of lung alveolar septae of B6 and TNF deficient mice, but not of LTβR deficient, micrograph 400×, H&E stained brain sections (E). semi-quantitative score of lung capillary (F–G). The data morphological data are from one representative out of 4–5 mice per group, and calculated date represent the mean±SD of n = 4 mice per group (n.s., not significant).

doi:10.1371/journal.pone.0002608.g003

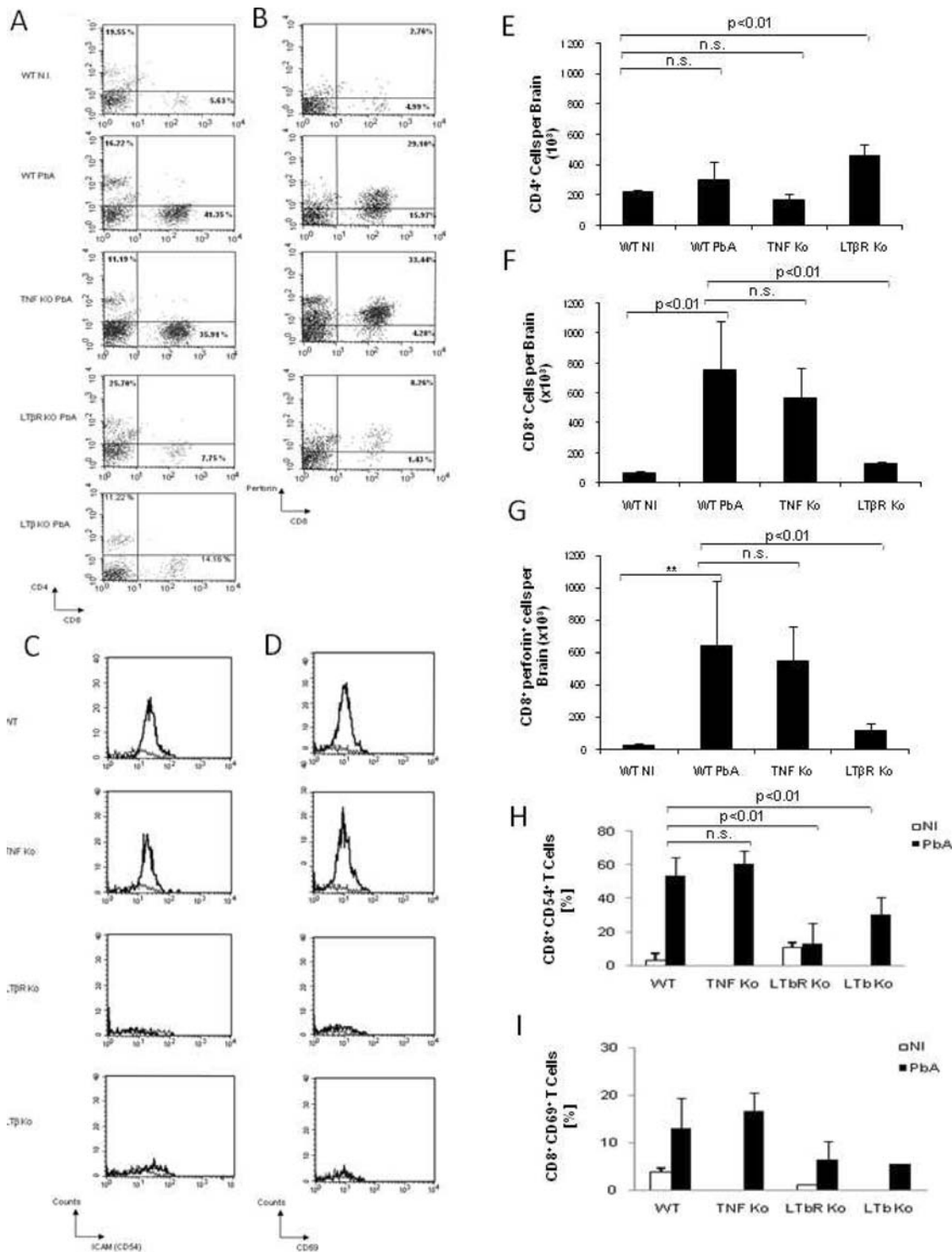


Figure 4. Reduced CD8⁺T lymphocytes infiltration in the brain of PbA-infected LTbR deficient mice. Flow cytometric analyses of brain-sequestered leukocytes from uninfected wild-type mice (WT NI), PbA-infected wild-type mice (WT PbA) and TNF deficient mice with severe ECM, and infected, ECM resistant LTb and LTbR deficient mice tested on the same day. Mice were infected with 10⁶ *P. berghei* ANKA parasitized red blood cells as in Fig. 1. Representative dot blots of CD4 and CD8 staining (A) CD8 and perforin double staining (B). Activation markers CD54 (C) and CD69 (D) on CD8⁺ cells are shown for non infected (thin line) and PbA infected (thick line) WT, TNF-, LTbR- and LTb-deficient mice, as indicated. Bargraphs of CD4⁺ (E), CD8⁺ (F), CD8⁺ Perforin⁺ (G), CD8⁺ CD54⁺ (H), and CD8⁺ CD69⁺ (I) lymphocytes represent the mean ± SD of n = 3–4 pools of 3–4 mice per group, and are from one representative of two independent experiments (n.s., not significant). doi:10.1371/journal.pone.0002608.g004

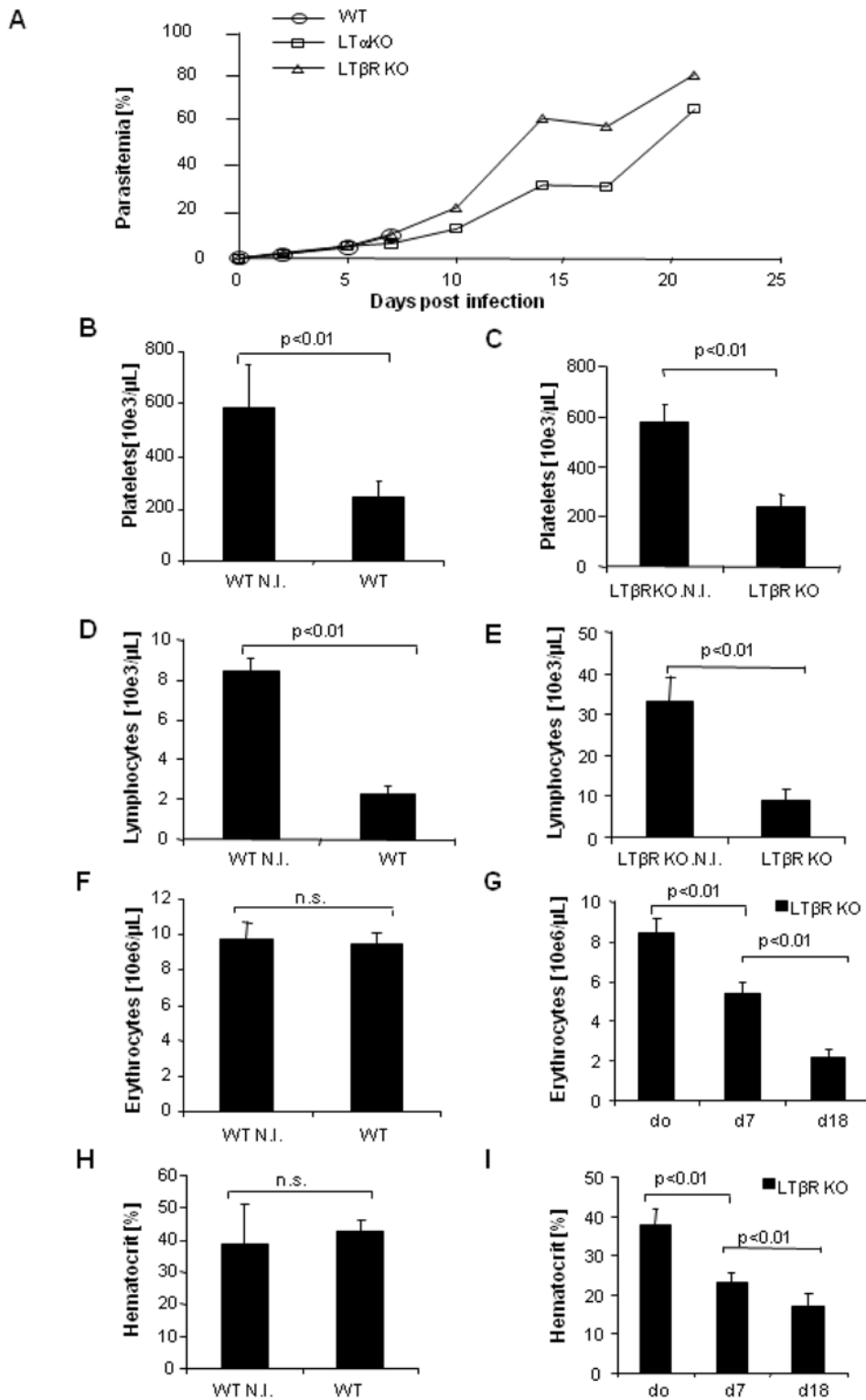


Figure 5. Parasitaemia and hematological alterations in LT β R deficient mice. The percentage of parasitized erythrocytes in the peripheral blood was determined up to day 22 for ECM resistant mice (A) after infection with 10^6 red blood cells parasitized by EGFP expressing *P. berghei* ANKA, by flow cytometry analysis of GFP fluorescent erythrocytes. Total platelet, lymphocyte and erythrocyte counts and hematocrit were determined in the peripheral blood of non infected (N.I.) and 7 day infected C57BL/6 and LT β R deficient mice (B–I). Anemia develops in LT β R deficient mice on day 18 after infection (I). The data represent the mean \pm SD of n = 5–12 mice per group from two independent experiments (n.s.; not significant). doi:10.1371/journal.pone.0002608.g005

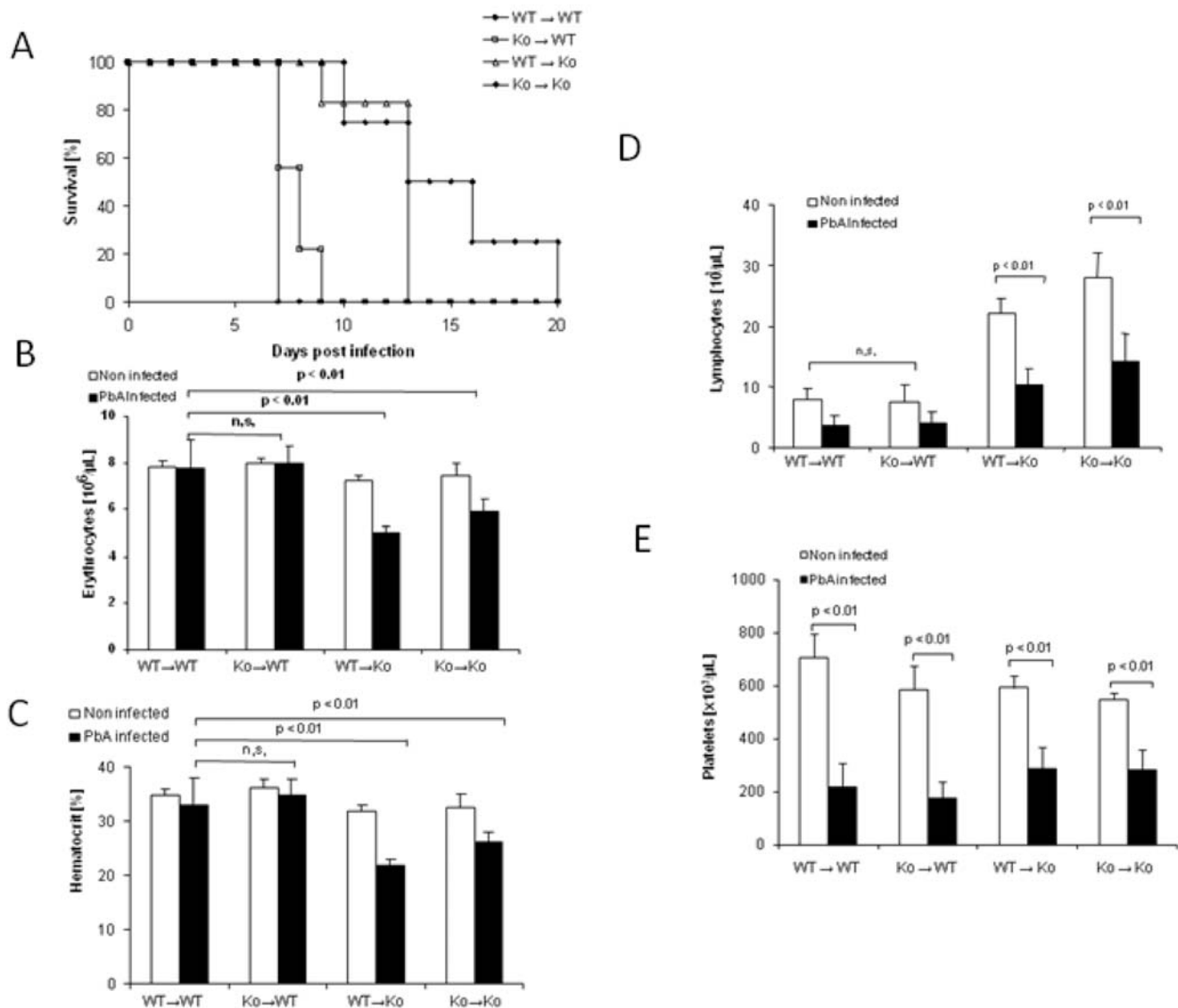


Figure 6. LTβR expressed on radioresistant stromal cells is critical for the development of ECM. C56BL/6 (WT) or LTβR deficient (KO) recipient mice were lethally irradiated and reconstituted with bone marrow cells from WT or KO mice as indicated (donor BM→recipient mice). The resulting WT→WT, WT→KO, KO→WT and KO→KO chimeric mice were infected with 10⁶ parasitized erythrocytes and survival was recorded (A). Hematological parameters such as erythrocyte counts (B), hematocrit (C), lymphocyte (D) and platelet (E) counts were determined on day 7 in naive and *P. berghei Anka* (PbA) infected mice. The data represent the mean±SD of n=5 mice per group (n.s., not significant). doi:10.1371/journal.pone.0002608.g006

Discussion

The present data demonstrate that interruption of LTβR signaling abrogates the microvascular disease leading to fatal ECM, which sheds a new light on the pathogenesis of cerebral malaria. Indeed, since LTα and TNFR2 signaling are also required for ECM development, we propose that both functional TNFR2 and LTβR axes are required for the development of microvascular pathology resulting in fatal ECM. The disruption of either axis prevents cerebral microvascular alterations, indicating that the two signaling pathways are non-redundant.

Signaling through TNF receptors activate the classic NF-κB/RelA pathway mediated by the inhibitors IκB-α, -β and -ε, leading to the expression of a large number of genes involved in inflammatory responses, cell adhesion or cell proliferation. In addition to the classic NF-κB/RelA pathway, LTβR signaling

activates NF-κB through an alternative, non-canonical NIK-IKK1-dependent route that results in the activation of RelB/NF-κB2. The alternative pathway NF-κB is activated by a limited set of receptors including LTβR, CD27, CD40, BAFFR, RANK, but not by TNF receptors. A recent study identified p100 as a fourth IκB protein that is required and sufficient for non-canonical NF-κB signaling downstream of NIK and IKK1, while it acts also as a signal transducer of NF-κB/RelA [26]. P100 was proposed as an integrator, involved in a cross-talk between canonical and non-canonical NF-κB inducing signaling that result in qualitative changes in the expression of inflammatory genes [26]. Examples of dual requirement for TNFR and LTβR stimulation were described for the in vitro generation of fibroblast reticular cells from lymph node tissue [27].

Although LTα deficient mice are resistant to ECM, LTβ deficient mice were slightly less protected and absence of LIGHT

did not prevent ECM. A similar apparent discrepancy, with milder phenotype for either LT β or LIGHT deficient mice as compared to LT α or LT β R deficient mice, was reported previously for lymphoid organogenesis [18]. Evidence for a cooperative role for LIGHT and LT β , existence of a weak LT α 3-LT β R interaction or of an additional ligand for LT β R were proposed [18]. Here, LIGHT, another LT β R ligand appears to be redundant in pathogenesis of ECM to blood stage PbA infection.

We investigated several pathophysiological aspects of CM in LT β R-deficient mice and show that the absence of clinical signs of ECM is associated with normal cerebral perfusion as assessed by MRI. The in vivo imaging data correlated with absence of microvascular disease with accumulation of mononuclear cells, vascular leak, hemorrhage and inflammation in the brain. Further, platelet adherence to cerebrovascular endothelium was absent in LT β R-deficient mice (data not shown), which is an important factor in ECM development as reported before [28]. Further pulmonary microvascular damage with alveolitis, plasma and erythrocyte leak in the alveolar space seen in control mice was also reduced in LT β R-deficient mice. Therefore, PbA induced microvascular damage in both lungs and brain is LT β R signaling dependent.

A previous report demonstrated a sex dependence of LT β R deficient mice infected with *Plasmodium chabaudi* [29], therefore we investigated whether males and females LT β R deficient mice have a differential susceptibility to PbA infection. However, we did not find any difference in susceptibility of male and female LT β R deficient mice to PbA infection unlike that reported for *P. chabaudi* infection [29].

Since members of the TNF family are involved in lymphoid organogenesis, we next questioned whether ECM resistance might be related to lymphoid organ structure and function. ECM resistant LT α , LT α β or LT β R deficient mice lack lymph node (LN) formation, while partially protected LT β deficient mice retain mesenteric LNs and in some cases cervical LNs, and intact lymphoid organs develop in the ECM sensitive LIGHT deficient mice [18]. Therefore, although absence of LT β R led to a severe defect in LN organogenesis, mice singly deficient for either LT β or LIGHT retained mesenteric LN, suggesting a redundancy or partial compensation of the two ligands. Bone marrow reconstitution is classically used to separate the effects on lymphoid organogenesis from the functional defects in adult mice. Wild-type bone marrow reconstitution in TNF/LT α deficient mice, that corrects immunodeficiency but not LN formation [24], could not restore their sensitivity to ECM [10]. Although the potential contribution of radiation-resistant brain endothelial cells, microglial cells or astrocytes as sources of LT α was proposed, the involvement of immune defects such as LN formation cannot be ruled out. We thus investigated in more details the inflammatory and hematological responses to PbA infections.

LT β R deficient mice, similar to wild-type mice, showed thrombocytopenia and decreased lymphocyte counts at day 7 when mice show signs of incipient CM, together with a slight anemia and slight increase in parasitaemia, that further increased thereafter. Therefore, disruption of LT β R signaling while protecting from ECM development, had no strong effect on the typical hematological / inflammatory response to PbA infection in mice. Further, absence of LT α or LT β R did not interfere with the progression of blood stage infection, and LT α or LT β R deficient mice succumb within 3 weeks of severe parasitaemia and anaemia.

Recent investigations demonstrated a potential for innate immune mechanisms directed against *Plasmodium* parasites to contribute to pathology and protection from malaria [30]. Several cell types such as DC, macrophages, $\gamma\delta$ T, NK and NKT cells contribute to the innate response [31]. Among them, non

lymphoid hematopoietic cells, but also follicular dendritic cells and stroma cells express LT β R. Both human and murine DC are activated by blood stage parasites in a TLR9 dependent manner [32], which is possibly mediated by hemozoin derived from infection with the human parasites [33]. NK cell are an important source of IFN γ and disruption of IFN γ signaling or NK cell depletion leads to increased parasitaemia and higher mortality in mouse models of malaria [31,34]. We have recently shown that macrophage derived IL-18 is required for NK cell activation by *P. falciparum* infected erythrocytes resulting in IFN γ production, which depends on IL18R/MyD88 signaling on both macrophages and NK cells [35]. However, TLR signaling of NK cells is dispensable for their activation [35]. We extensively investigated the role of TLR and their adaptor proteins, in the control of ECM, but found that TLR signaling does not contribute to the development of ECM induced by blood-stage PbA [36] while others suggested TLR9-MyD88 dependence of ECM development.

CD8⁺ T cells were recently shown to be the primary effectors of CM in the *Plasmodium berghei* ANKA mouse model, although their precise mechanism of action remains unresolved [37]. CD8⁺ T cells may mediate circulatory shock, vascular permeability changes, and edema in the brain during PbA infection [38]. We therefore investigated whether absence of LT β R affects T cell response to PbA induced ECM, and whether the effect is direct. We show a clear reduction in brain-infiltrating CD8⁺ cells in ECM resistant LT β R mice. The low recruitment and activation of CD8⁺ T cells in the brain of LT β R deficient mice may be linked to a defective production of CXCR3 ligands CXCL9, 10, 11, essential for T cell migration to inflamed tissues, that are reduced in the absence of LT β R [11]. Absence of LT β R seemed to have little incidence on the effector properties of the sequestered CD8⁺ T cell which expressed perforin, although the overall population of perforin⁺ CD8 cells was clearly reduced in LT β R deficient mice, due to a sharp decrease in CD8⁺ population recruited in the brain. ICAM⁺ and CD69⁺ CD8⁺ T cells were also largely reduced in the brain of PbA infected LT β R deficient mice. LT α / β expressing CD8⁺ T cells might participate directly in the microvascular pathology, through an interaction with LT β R expressed on endothelial cells, leading to cell activation, expression of adhesion molecules or cytokine secretion. The diminished recruitment and activation of CD8⁺ T cells in the brain of LT β R deficient mice may therefore be responsible for protection from ECM development.

Bone marrow irradiation chimera experiments revealed that LT β R expression on radioresistant resident stromal cells is essential for the development of ECM. Reconstitution of LT β R deficient mice with wild-type bone marrow did not confer sensitivity to ECM. Therefore, the data suggest that LT β R expressed on endothelial cells might be critical, and their absence may prevent the recruitment of CD8 lymphocytes into the brain and microvascular pathology.

The clinical relevance of the findings in mice are under investigation for gene polymorphism of the TNF/LT α locus [39]. Association between TNF/LT α polymorphism and increased risk of cerebral malaria has been reported [40–43], however more investigations are necessary to fully decipher the molecular bases of the link between disease manifestation and TNF/LT α polymorphism.

In conclusion, the data suggest that both functional LT β R and TNFR2 signaling are required and non-redundant for the development of microvascular pathology resulting in fatal ECM. The disruption of either axis prevents cerebral microvascular disease.

Materials and Methods

Mice

Mice deficient for TNF [44], LT α [45], LT β [46] and LT $\alpha\beta$ [47], TNFR1 [48], TNFR2 [49], LT β R [17] or LIGHT deficient mice [18] were bred in the animal facility of the Transgenose Institute (CNRS, Orleans). All mice were on C57BL/6J genetic background (back-crossed at least 10 times, beside TNFR2 deficient mice that were back-crossed 2 times) and wild-type control C57BL/6J (WT) mice were used. For experiments, adult (7–10 weeks old) mice were kept in filtered-cages in P2 animal facility. All animal experiments complied with the French Government's ethical and animal experiments regulations.

Experimental malaria infection

A cloned line of *Plasmodium berghei* ANKA (PbA) stably transfected with GFP was obtained from Dr. A Waters [50]. Mice were infected by intraperitoneal injection of 10^6 parasitized erythrocytes as described before [9]. Mice were observed daily for clinical neurological signs of ECM culminating in ataxia, paralysis and coma. Parasitaemia was analyzed by flow cytometry [22] at various time point and hematological parameters were assessed as indicated. Before succumbing to neurological symptoms, mice were killed for histological analysis of the brain, lung and liver.

Parasitaemia

Parasitaemia was assessed in 2 μ l of blood collected from the tail vein at different time points post-infection with EGFP-*Plasmodium berghei* ANKA. Blood was diluted in 2 ml of PBS containing 0.5% BSA and fluorescent cells analyzed by FACScan flow cytometer LSR (Becton Dickinson, Grenoble, France) using CellQuest software (Becton Dickinson, Grenoble, France).

Hematology

Blood was drawn into tubes containing EDTA (Vacutainer; Becton, Grenoble, France) as indicated and hematological parameters determined using 5-part-differential hematology analyzer MS 9.5 (Melet Schloesing Laboratoires, France).

Histology

For histological analysis, the mice were perfused under anesthesia with saline and the brain, lung, and liver from *P. berghei* ANKA infected mice were fixed in 4% phosphate-buffered-saline formaldehyde for 72 h as described before [9]. Three μ m sections were stained with haematoxylin and eosin. CNS microvascular obstruction, erythrocyte accumulation in alveoli, thickening of alveolar septae were quantified using a semi-quantitative score with increasing severity of changes (0–5) by two independent observers including a trained pathologist (BR) as described [9].

Bone marrow chimera

C57BL/6J (WT) mice and LT β R deficient mice received lethal body irradiation (8 Gy). Fresh, nucleated bone marrow cells (5×10^6 per mouse) were injected into the lateral tail vein of the recipient mice 24 hours after irradiation. The reconstituted mice were used at 2 months after bone marrow transplantation [24,25].

Assessment of vascular leak

Mice were injected intravenously (i.v) with 0.2 ml of 1% Evans blue (Sigma-Aldrich) on day 7, shortly before the death of the wild type mice. One hour later, mice were sacrificed and the coloration of brain was assessed. Brain and lung extravasation in formamide (Sigma-Aldrich) was evaluated by absorbance at 610 nm of the

tissue extracts as an indicator of increased capillary permeability [9].

Brain imaging using magnetic resonance imaging (MRI)

MRI experiments were performed in a horizontal 9.4 T/20-ECM Bruker Biospec MR system (Bruker Biospin, Wissembourg, France) equipped with gradients capable of switching 950 mT/m in 50 μ s. A 12 elements linear birdcage coil (Bruker Biospin) with inner diameter of 35 mm and length 60 mm has been used to achieve uniform excitation and reception.

A custom-built stereotaxic head holder was used to fix the animals into the birdcage coil (see below). The mice were anaesthetized with isoflurane (1.5–2.5%) in an O₂/N₂O 1:1 mixture applied with a face mask allowing free breathing. Respiration was monitored using a balloon taped to the abdomen and connected to a pressure transducer (SA Instruments, Inc., Stony Brook, NY, USA). The mice body temperature was kept at 37 ± 0.5 °C throughout the experiment, using warm water circulation.

Preparatory anatomical sagittal MR images were performed using a MSME (multi-slices, multi-echoes) sequence, with the following parameters: RARE factor = 8, TR/TE_{eff} = 4000/46 ms, FOV = 20×20 mm², matrix = 128×128 , 1 slice 1 mm thickness, number of averages (NA) = 1, experimental time = 1 min.

Brain lesions and global changes in tissue structure have been accessed by T₂ weighted (T2w) MR images using a MSME sequence, with the following parameters: RARE factor = 8, TR/TE_{eff} = 5000/46 ms, FOV = 17×17 mm², matrix = 256×192 (zero-filled to 256×256), 37 axial slices 0.5 mm thickness, NA = 8, experimental time = 16 min.

Measurements of vascular cerebral blood flow was performed by MR angiography (MRA) using a Fast Low Angle Shot (FLASH) sequence, with the following parameters: FOV = 14×14 mm², matrix = 128×128 , TR/TE = 30/5 ms, 51 axial slices 0.3 mm thickness, NA = 4, experimental time = 13 min. Angiograms were produced by generating maximum intensity projections (MIP) after interpolating raw data to obtain an isotropic resolution ($109 \mu\text{m}$)³. Image analysis and processing were performed with the public domain software Image J (NIH, <http://rsb.info.nih.gov/ij>).

Isolation of brain-sequestered leukocytes

Mice with neurological symptoms of ECM were anaesthetized (at day 7–8) and perfused with 10 ml of PBS/EDTA 0.02% intracardiac to remove circulating red blood cells and leukocytes from the brain as described.[20] Brains were removed and homogenized gently (30 sec at 4000 rpm) using the sterile disposable homogenization system Dispomix (Medic Tools AG, 6300-Zug, Switzerland) in RPMI 1640 medium containing 2% FCS. Tissue-cell homogenates were passed through a nylon cell strainer (100 μ m; Becton Dickinson Grenoble, France) and centrifuged at 400 g for 10 minutes. The mononuclear cells were then separated over a 30% Percoll gradient (Amersham Biosciences AB, Uppsala, Sweden). Residual red blood cells were lysed by hypotonic shock in ammonium chloride-potassium lysis buffer.

Flow cytometry analysis (FACS)

Brain-sequestered cells were collected, washed and saturated with mouse serum prior to the staining with fluorescence labelled antibodies for 30 minutes. The cells were then phenotyped by flow cytometry. T cells were identified by their forward side scatter and with the use of the following antibodies: rat anti-mouse CD4 conjugated to fluorescein isothiocyanate (FITC) (clone GK1.5; Pharmingen San Diego, CA), rat anti-mouse CD8 α conjugated to allophycocyanin (APC) (clone 53-6.7, Pharmingen San Diego,

CA), rat anti-mouse Perforin conjugated to phycoerythrin (PE) (clone JAW246, eBioscience San Diego, CA), rat anti-mouse CD69 conjugated to phycoerythrin (PE) (clone H1.F3, Becton-Dickinson, Grenoble France), rat anti-mouse CD54 conjugated to PE (clone 3E2, Becton-Dickinson, Grenoble France) and isotype-matched control antibodies (Becton-Dickinson, Grenoble France). For each sample, 10000 cells were scored. Data were analyzed using a LSR II-Flow cytometer and CellQuest software (Becton-Dickinson, Grenoble France).

Statistical analysis

Data are presented as mean values and standard deviation (SD) indicated by error bars, if not otherwise indicated. Statistical significance was determined with Graph Pad Prism software (version 4.0, San Diego, CA). Differences between multiple groups were analyzed for statistical significance by means of one way non-parametric ANOVA test followed by Dunn's multiple comparison test for some data or Logrank Test, for others we used Kruskal-Wallis test followed by Dunn's multiple comparison test. P values of <0.05 were considered statistically significant.

Supporting Information

Video S1 3D MRA Video 1 : Non-infected C57BL/6 wild-type mouse. Three-dimensional (3D) Magnetic Resonance Angiography (MRA) movies of non-infected wild-type C57BL/6, and wild-type or mice deficient for TNF, LT α LT β , or LT β R 7 days post infection with 10e6 *P. berghei* ANKA parasitized red blood cells. Video 1 : Non-infected C57BL/6 wild-type mouse. Compared to 2D views, 3D MRA allows a better observation of the vascular blood flow perturbations in wild-type and TNF-KO mice. Before 3D reconstruction, two dimensional angiograms (2D-MRA) were produced by Maximum Intensity Projections (MIP) as described in the Methods section. Movies were created by rotating the 2D-MRA views at different angles (using steps of 20 degrees). Image analysis and processing (including 3D MRA movies) were performed with the public domain software ImageJ (NIH, <http://rsb.info.nih.gov/ij>). Found at: doi:10.1371/journal.pone.0002608.s001 (1.71 MB AVI)

Video S2 3D MRA Video 2 : PbA-infected C57BL/6 mouse. Three-dimensional (3D) Magnetic Resonance Angiography (MRA) movies of non-infected wild-type C57BL/6, and wild-type or mice deficient for TNF, LT α LT β , or LT β R 7 days post infection with 10e6 *P. berghei* ANKA parasitized red blood cells. Video 2 : PbA-infected C57BL/6 mouse. Compared to 2D views, 3D MRA allows a better observation of the vascular blood flow perturbations in wild-type and TNF-KO mice. Before 3D reconstruction, two dimensional angiograms (2D-MRA) were produced by Maximum Intensity Projections (MIP) as described in the Methods section. Movies were created by rotating the 2D-MRA views at different angles (using steps of 20 degrees). Image analysis and processing (including 3D MRA movies) were performed with the public domain software ImageJ (NIH, <http://rsb.info.nih.gov/ij>). Found at: doi:10.1371/journal.pone.0002608.s002 (1.92 MB AVI)

Video S3 3D MRA Video 3 : PbA-infected TNF ko mouse. Three-dimensional (3D) Magnetic Resonance Angiography (MRA) movies of non-infected wild-type C57BL/6, and wild-type

or mice deficient for TNF, LT α LT β , or LT β R 7 days post infection with 10e6 *P. berghei* ANKA parasitized red blood cells. Video 3 : PbA-infected TNF ko mouse. Compared to 2D views, 3D MRA allows a better observation of the vascular blood flow perturbations in wild-type and TNF-KO mice. Before 3D reconstruction, two dimensional angiograms (2D-MRA) were produced by Maximum Intensity Projections (MIP) as described in the Methods section. Movies were created by rotating the 2D-MRA views at different angles (using steps of 20 degrees). Image analysis and processing (including 3D MRA movies) were performed with the public domain software ImageJ (NIH, <http://rsb.info.nih.gov/ij>). Found at: doi:10.1371/journal.pone.0002608.s003 (1.92 MB AVI)

Video S4 3D MRA Video 4 : PbA-infected LT α β ko mouse. Three-dimensional (3D) Magnetic Resonance Angiography (MRA) movies of non-infected wild-type C57BL/6, and wild-type or mice deficient for TNF, LT α LT β , or LT β R 7 days post infection with 10e6 *P. berghei* ANKA parasitized red blood cells. Video 4 : PbA-infected LT α β ko mouse. Compared to 2D views, 3D MRA allows a better observation of the vascular blood flow perturbations in wild-type and TNF-KO mice. Before 3D reconstruction, two dimensional angiograms (2D-MRA) were produced by Maximum Intensity Projections (MIP) as described in the Methods section. Movies were created by rotating the 2D-MRA views at different angles (using steps of 20 degrees). Image analysis and processing (including 3D MRA movies) were performed with the public domain software ImageJ (NIH, <http://rsb.info.nih.gov/ij>). Found at: doi:10.1371/journal.pone.0002608.s004 (1.74 MB AVI)

Video S5 3D MRA Video 5 : PbA-infected LT β R ko mouse. Three-dimensional (3D) Magnetic Resonance Angiography (MRA) movies of non-infected wild-type C57BL/6, and wild-type or mice deficient for TNF, LT α LT β , or LT β R 7 days post infection with 10e6 *P. berghei* ANKA parasitized red blood cells. Video 4 : PbA-infected LT β R ko mouse. Compared to 2D views, 3D MRA allows a better observation of the vascular blood flow perturbations in wild-type and TNF-KO mice. Before 3D reconstruction, two dimensional angiograms (2D-MRA) were produced by Maximum Intensity Projections (MIP) as described in the Methods section. Movies were created by rotating the 2D-MRA views at different angles (using steps of 20 degrees). Image analysis and processing (including 3D MRA movies) were performed with the public domain software ImageJ (NIH, <http://rsb.info.nih.gov/ij>). Found at: doi:10.1371/journal.pone.0002608.s005 (1.71 MB AVI)

Acknowledgments

The authors are grateful to Dr. Analbery Monteiro for thorough analysis of the MRI data.

Author Contributions

Conceived and designed the experiments: RM LR JB BR VQ GG DT NH MF VB PL SS AH. Performed the experiments: BD DT MF VB PL LF AH HB. Analyzed the data: RM KP LR JB BR VQ BD GG DT NH MF VB PL LF SS AH HB. Contributed reagents/materials/analysis tools: RM KP LR JB BD NH LF SS HB. Wrote the paper: KP BR VQ GG.

References

1. Miller LH, Good MF, Milon G (1994) Malaria pathogenesis. *Science* 264: 1878–1883.
2. Idro R, Jenkins NE, Newton CR (2005) Pathogenesis, clinical features, and neurological outcome of cerebral malaria. *Lancet Neurol* 4: 827–840.
3. Hunt NH, Grau GE (2003) Cytokines: accelerators and brakes in the pathogenesis of cerebral malaria. *Trends Immunol* 24: 491–499.
4. Schofield L, Grau GE (2005) Immunological processes in malaria pathogenesis. *Nat Rev Immunol* 5: 722–735.

5. Grau GE, Taylor TE, Molyneux ME, Wirima JJ, Vassalli P, et al. (1989) Tumor necrosis factor and disease severity in children with falciparum malaria. *N Engl J Med* 320: 1586–1591.
6. Kern P, Hemmer CJ, Van Damme J, Gruss HJ, Dietrich M (1989) Elevated tumor necrosis factor alpha and interleukin-6 serum levels as markers for complicated *Plasmodium falciparum* malaria. *Am J Med* 87: 139–143.
7. Kwiatkowski D, Hill AV, Sambou I, Tsumasi P, Castracane J, et al. (1990) TNF concentration in fatal cerebral, non-fatal cerebral, and uncomplicated *Plasmodium falciparum* malaria. *Lancet* 336: 1201–1204.
8. Grau GE, Fajardo LF, Piguet PF, Allet B, Lambert PH, et al. (1987) Tumor necrosis factor (cachectin) as an essential mediator in murine cerebral malaria. *Science* 237: 1210–1212.
9. Rudin W, Eugster HP, Bordmann G, Bonato J, Muller M, et al. (1997) Resistance to cerebral malaria in tumor necrosis factor-alpha/beta-deficient mice is associated with a reduction of intercellular adhesion molecule-1 up-regulation and T helper type 1 response. *Am J Pathol* 150: 257–266.
10. Engwerda CR, Mynott TL, Sawhney S, De Souza JB, Bickle QD, et al. (2002) Locally up-regulated lymphotoxin alpha, not systemic tumor necrosis factor alpha, is the principle mediator of murine cerebral malaria. *J Exp Med* 195: 1371–1377.
11. Gommerman JL, Browning JL (2003) Lymphotoxin/light, lymphoid microenvironments and autoimmune disease. *Nat Rev Immunol* 3: 642–655.
12. Fu YX, Chaplin DD (1999) Development and maturation of secondary lymphoid tissues. *Annu Rev Immunol* 17: 399–433.
13. Ware CF (2005) Network communications: lymphotoxins, LIGHT, and TNF. *Annu Rev Immunol* 23: 787–819.
14. Hehlgans T, Pfeffer K (2005) The intriguing biology of the tumour necrosis factor/tumour necrosis factor receptor superfamily: players, rules and the games. *Immunology* 115: 1–20.
15. Flynn JL, Goldstein MM, Chan J, Tricbold KJ, Pfeffer K, et al. (1995) Tumor necrosis factor-alpha is required in the protective immune response against *Mycobacterium tuberculosis* in mice. *Immunity* 2: 561–572.
16. Stoelcker B, Hehlgans T, Weigl K, Bluethmann H, Grau GE, et al. (2002) Requirement for tumor necrosis factor receptor 2 expression on vascular cells to induce experimental cerebral malaria. *Infect Immun* 70: 5857–5859.
17. Futterer A, Mink K, Luz A, Kosco-Vilbois MH, Pfeffer K (1998) The lymphotoxin beta receptor controls organogenesis and affinity maturation in peripheral lymphoid tissues. *Immunity* 9: 59–70.
18. Scheu S, Alferink J, Potzel T, Barchet W, Kalin U, et al. (2002) Targeted disruption of LIGHT causes defects in costimulatory T cell activation and reveals cooperation with lymphotoxin beta in mesenteric lymph node genesis. *J Exp Med* 195: 1613–1624.
19. Penet MF, Viola A, Confort-Gouny S, Le Fur Y, Duhamel G, et al. (2005) Imaging experimental cerebral malaria in vivo: significant role of ischemic brain edema. *J Neurosci* 25: 7352–7358.
20. Belnoue E, Kayibanda M, Vigario AM, Deschemin JC, van Rooijen N, et al. (2002) On the pathogenic role of brain-sequestered alphabeta CD8+ T cells in experimental cerebral malaria. *J Immunol* 169: 6369–6375.
21. Ntcheu JBO, Combadiere C, Tefit M, Scilhean D, Mazier D, et al. (2003) Perforin-dependent brain-infiltrating cytotoxic CD8+ T lymphocytes mediate experimental cerebral malaria pathogenesis. *Journal of Immunology* 170: 22221–22228.
22. Voza TVA, Belnoue E, Gruner AC, Deschemin JC, Kayibanda M, et al. (2005) Species-specific inhibition of cerebral malaria in mice coinfecting with *Plasmodium* spp. *Infect Immun* 73: 4777–4786.
23. Grau GEPP, Gretener D, Vesin C, Lambert PH (1988) Immunopathology of thrombocytopenia in experimental malaria. *Immunology* 65: 501–506.
24. Muller M, Eugster HP, Le Hir M, Shakhov A, Di Padova F, et al. (1996) Correction or transfer of immunodeficiency due to TNF-LT alpha deletion by bone marrow transplantation. *Mol Med* 2: 247–255.
25. Ryffel B, Di Padova F, Schreier MH, Le Hir M, Eugster HP, et al. (1997) Lack of type 2 T cell-independent B cell responses and defect in isotype switching in TNF-lymphotoxin alpha-deficient mice. *J Immunol* 158: 2126–2133.
26. Basak SKH, Kearns JD, Tergaonkar V, O'Dea E, Werner SL, et al. (2007) A fourth IkkappaB protein within the NF-kappaB signaling module. *Cell* 128: 369–381.
27. Katakai THT, Sugai M, Gonda H, Shimizu A (2004) Lymph node fibroblastic reticular cells construct the stromal reticulum via contact with lymphocytes. *Journal of Experimental Medicine* 200: 783–795.
28. von Zur Muhlen C, Sibson NR, Peter K, Campbell SJ, Wilainam P, et al. (2008) A contrast agent recognizing activated platelets reveals murine cerebral malaria pathology undetectable by conventional MRI. *J Clin Invest* 118: 1198–1207.
29. Wunderlich F, Dkhil MA, Mehnert LI, Braun JV, El-Khadragy M, et al. (2005) Testosterone responsiveness of spleen and liver in female lymphotoxin beta receptor-deficient mice resistant to blood-stage malaria. *Microbes Infect* 7: 399–409.
30. Hall NCJ (2005) Comparative genomics of malaria parasites. *Curr Opin Genet Dev* 15: 609–613.
31. Stevenson MM, Riley EM (2004) Innate immunity to malaria. *Nat Rev Immunol* 4: 169–180.
32. Pichyangkul SGM, Miller RS, Lyon JA, Angov E, Tongtawe P, et al. (2004) Pre-clinical evaluation of the malaria vaccine candidate P. falciparum MSP1(42) formulated with novel adjuvants or with alum. *Vaccine* 22: 3831–3840.
33. Coban C, Ishii KJ, Kawai T, Hemmi H, Sato S, et al. (2005) Toll-like receptor 9 mediates innate immune activation by the malaria pigment hemozoin. *J Exp Med* 201: 19–25.
34. Amani V, Vigario AM, Belnoue E, Marussig M, Fonseca L, et al. (2000) Involvement of IFN-gamma receptor-mediated signaling in pathology and anti-malarial immunity induced by *Plasmodium berghei* infection. *Eur J Immunol* 30: 1646–1655.
35. Baratin M, Roctynck S, Lepolard C, Falk C, Sawadogo S, et al. (2005) Natural killer cell and macrophage cooperation in MyD88-dependent innate responses to *Plasmodium falciparum*. *Proc Natl Acad Sci U S A* 102: 14747–14752.
36. Togbe DSL, Grau GE, Schnyder B, Boissay V, Charron S, et al. (2007) Murine Cerebral Malaria development is independent of Toll-Like signaling. *Am J Pathol* 170: 1640–1648.
37. Renia L, Potter SM, Mauduit M, Rosa DS, Kayibanda M, et al. (2006) Pathogenic T cells in cerebral malaria. *Int J Parasitol* 36: 547–554.
38. Chang WL, Jones SP, Lefler DJ, Welbourne T, Sun G, et al. (2001) CD8(+)-T-cell depletion ameliorates circulatory shock in *Plasmodium berghei*-infected mice. *Infect Immun* 69: 7341–7348.
39. Flori L, Delahaye NF, Iraqi FA, Hernandez-Valladares M, Fumoux F, et al. (2005) TNF as a malaria candidate gene: polymorphism-screening and family-based association analysis of mild malaria attack and parasitemia in Burkina Faso. *Genes Immun* 6: 472–480.
40. McGuire WHA, Allsopp CE, Greenwood BM, Kwiatkowski D (1994) Variation in the TNF-alpha promoter region associated with susceptibility to cerebral malaria. *Nature* 371: 508–510.
41. Wattavidanage JCR, Perera KL, Munasingha A, Bandara S, McGuinness D, et al. (1999) TNFalpha*2 marks high risk of severe disease during *Plasmodium falciparum* malaria and other infections in Sri Lankans. *Clin Exp Immunol* 115: 350–355.
42. Aidoo MMP, Kolczak MS, Terlouw DJ, ter Kuile FO, Nahlen B, et al. (2001) Tumor necrosis factor-alpha promoter variant 2 (TNF2) is associated with pre-term delivery, infant mortality, and malaria morbidity in western Kenya: Asembo Bay Cohort Project IX. *Genet Epidemiol* 21: 201–211.
43. Gimenez FBdLS, Fernandez C, Pino P, Mazier D (2003) Tumor necrosis factor alpha in the pathogenesis of cerebral malaria. *Cell Mol Life Sci* 60: 1623–1635.
44. Marino MW, Dunn A, Grail D, Ingles M, Noguchi Y, et al. (1997) Characterization of tumor necrosis factor-deficient mice. *Proc Natl Acad Sci U S A* 94: 8093–8098.
45. De Togni P, Goellner J, Ruddle NH, Streeter PR, Fick A, et al. (1994) Abnormal development of peripheral lymphoid organs in mice deficient in lymphotoxin. *Science* 264: 703–707.
46. Alimzhanov MB, Kuprash DV, Kosco-Vilbois MH, Luz A, Turetskaya RL, et al. (1997) Abnormal development of secondary lymphoid tissues in lymphotoxin beta-deficient mice. *Proc Natl Acad Sci U S A* 94: 9302–9307.
47. Kuprash DV, Alimzhanov MB, Tumanov AV, Anderson AO, Pfeffer K, et al. (1999) TNF and lymphotoxin beta cooperate in the maintenance of secondary lymphoid tissue microarchitecture but not in the development of lymph nodes. *J Immunol* 163: 6575–6580.
48. Rothe J, Lesslauer W, Lotscher H, Lang Y, Koebel P, et al. (1993) Mice lacking the tumour necrosis factor receptor 1 are resistant to TNF-mediated toxicity but highly susceptible to infection by *Listeria monocytogenes*. *Nature* 364: 798–802.
49. Erickson SL, de Sauvage FJ, Kikly K, Carver-Moore K, Pitts-Meck S, et al. (1994) Decreased sensitivity to tumour-necrosis factor but normal T-cell development in TNF receptor-2-deficient mice. *Nature* 372: 560–563.
50. Franke-Fayard B, Janse CJ, Cunha-Rodrigues M, Ramesar J, Buscher P, et al. (2005) Murine malaria parasite sequestration: CD36 is the major receptor, but cerebral pathology is unlinked to sequestration. *Proc Natl Acad Sci U S A* 102: 11468–11473.